Characterization of anodes for lithium-ion batteries

R. M. Humana[1,2] · M. G. Ortiz[2,3] · J. E. Thomas[2] · S. G. Real[2,3] · M. Sedlarikova[4] · J. Vondrak[4] · A. Visintin[2]

Abstract The lithium-ion batteries are energy storage systems of high performance and low cost. They are employed in multiple portable devices, and these require the use of increasingly smaller and lighter batteries with high energy and power density, fast charging, and long service life. Moreover, these systems are promising for use in electric or hybrid vehicles. However, the lithium-ion battery still requires the improvement of the electrode material properties, such as cost, energy density, cycle life, safety, and environmental compatibility. These batteries use carbon as anode material, usually synthetic graphite, because of its high coulombic efficiency and acceptable specific capacity for the formation of intercalation compounds (LiC_6). In this paper, the methodology used to prepare and characterize the reversible and irreversible capacity and cyclic stability of graphite materials as anodes in lithium-ion batteries of commercial carbon and shungite carbon is presented. The results obtained using electrochemical techniques are discussed. These electrodes exhibited good activation process and high-rate dischargeability performance. For carbon and shungite electrodes, the maximum discharge capacity values were 259 and 170 mA h g^{-1}, respectively.

Dedicated to Professor Jose H. Zagal on the occasion of his 65th birthday.

✉ A. Visintin
visintinarnaldo2@gmail.com

[1] Centro de Investigaciones y Transferencia de Catamarca (CITCA), CONICET-UNCA, Prado 366, K4700AAP. San Fernando del Valle de Catamarca, Catamarca, Argentina

[2] Instituto de Investigaciones Fisicoquímicas Teóricas y Aplicadas (INIFTA), Facultad de Ciencias Exactas, Universidad Nacional de La Plata (UNLP), CCT La Plata-CONICET, CC 16, Suc. 4, 1900 La Plata, Argentina

[3] Centro de Investigación, Desarrollo en Ciencia y Tecnología de los Materiales (CITEMA), Facultad Regional La Plata, Universidad Tecnológica Nacional, Calle 60 y 124, La Plata, Argentina

[4] Department of Electrical and Electronic Technology, Faculty of Electrical Engineering and Communication, Brno University of Technology, Technicka 10, 616 00 Brno, Czech Republic

Introduction

The escalating demand for high-energy-density Li-ion batteries has led to increasing focus on finding alternatives to existing graphite anode materials, with higher storage capacities. Carbon has been applied as anode materials for lithium-ion batteries due to its low cost and high cycling stability. However, its low Li-storage capacity cannot satisfy the requirements of the electronic devices and electric vehicles to the battery. Silicon is regarded a promising alternative to the carbon materials because of its very high specific capacity of Li-storage [1–3]. However, the large volume change during lithium ion insertion/extraction process can induce enormous mechanical stress, and then leads to pulverization of the Si electrode materials and loss of electrical contact with current collector, which may result in decreasing in reversible capacity [4]. In fact, the poor cycling stability hinders its wide application in energy-storage batteries. The expanded efforts to improve the electrochemical improve the electrochemical performance of anodes, as discussed in detail in recently published papers [5–12].

Artificial graphite has been considered a very good high-powered anode material in the lithium-ion batteries, even with better electrochemical performance than natural graphite [13, 14]. Graphite has been widely used in different commercial applications because of their good properties, such as stability of the electrode/electrolyte interphase, the low and flat operating voltage, and the relatively high specific capacity [15]. Recently, many different types of artificial graphite materials (cokes, carbon fibers, mesocarbon microbeads (MCMBs)),

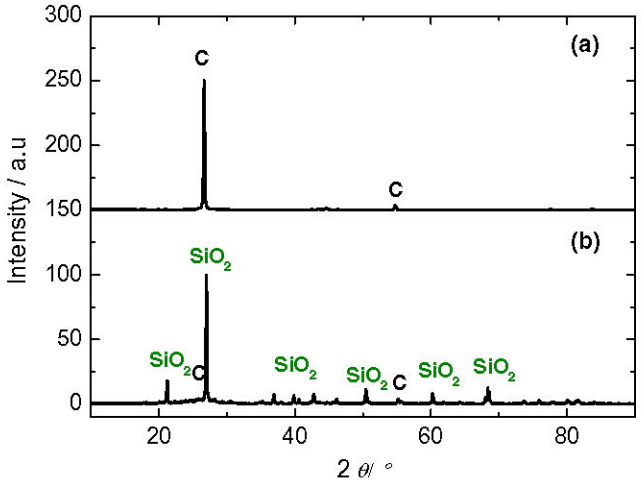

Fig. 1 XRD pattern of **a** commercial carbon and **b** shungite sample

Table 1 Composition values obtained by EDS technique

	C	Si	O
Weight % shungite	40.5	23.4	44.4
Weight % carbon	84.5	–	06.9

The concentration of Mg, Al, S, K, and Fe are less than 1 %

anthracite, etc. have been studied as anodes for high-power lithium-ion batteries [16].

In this work, the preparation and characterization, using physic and electrochemical techniques, of graphite materials and shungite carbon as anodes, for lithium-ion batteries, are presented. Shungite is a natural carbonaceous mineral, abundant in Russia with highly dispersed silicate mineral grains evenly distributed in the shungite carbon matrix. The structure and chemical composition of the materials were characterized by X-Ray diffraction (XRD), scanning electron microscopy (SEM), transmission electron microscopy (TEM), and thermogravimetric analysis (TGA). The electrochemical characterization was carried out using charge-discharge curves at different current densities, cyclic voltammetry, and electrochemical impedance spectroscopy (EIS) techniques.

Experimental

The crystal structure of the samples was characterized by XRD (Philips PW1700). SEM (FEI Quanta 650 FEG) along with the X-ray energy-dispersive spectroscopy (EDX) analysis was used to study the surface properties and chemical composition, respectively. TEM micrographs were acquired with a FEI Tecnai G2 F20. The TGA curves were recorded

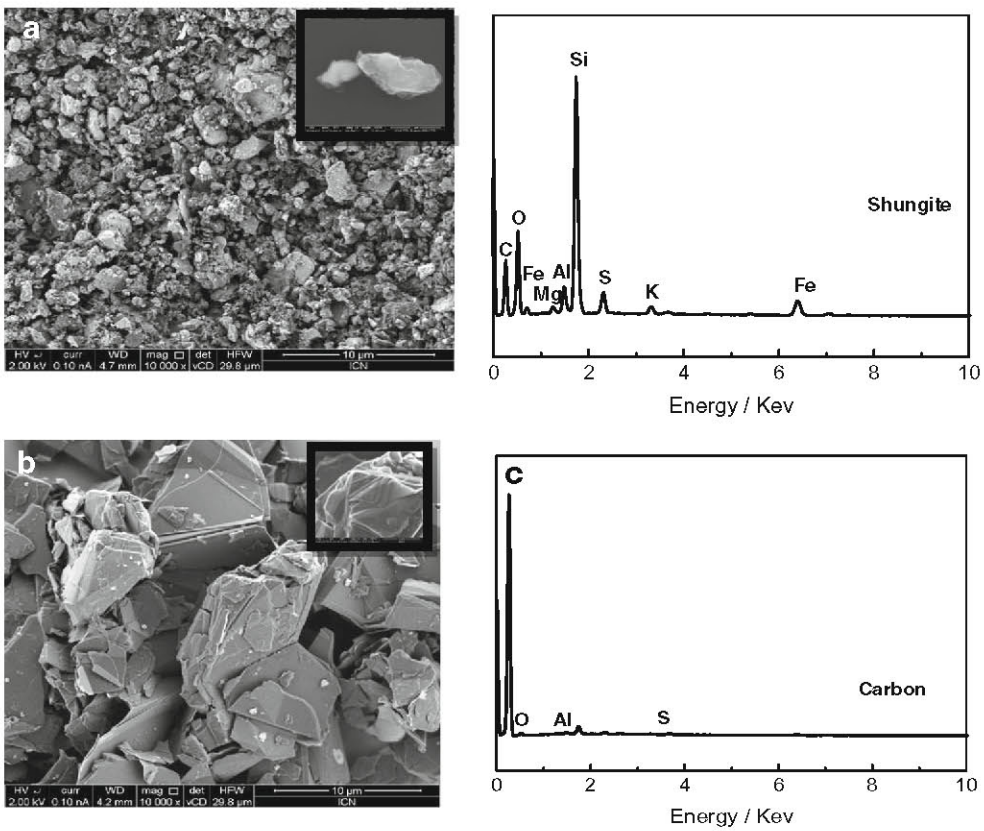

Fig. 2 SEM images and EDS spectrum: **a** shungite and **b** commercial carbon. With a magnification to observe the samples

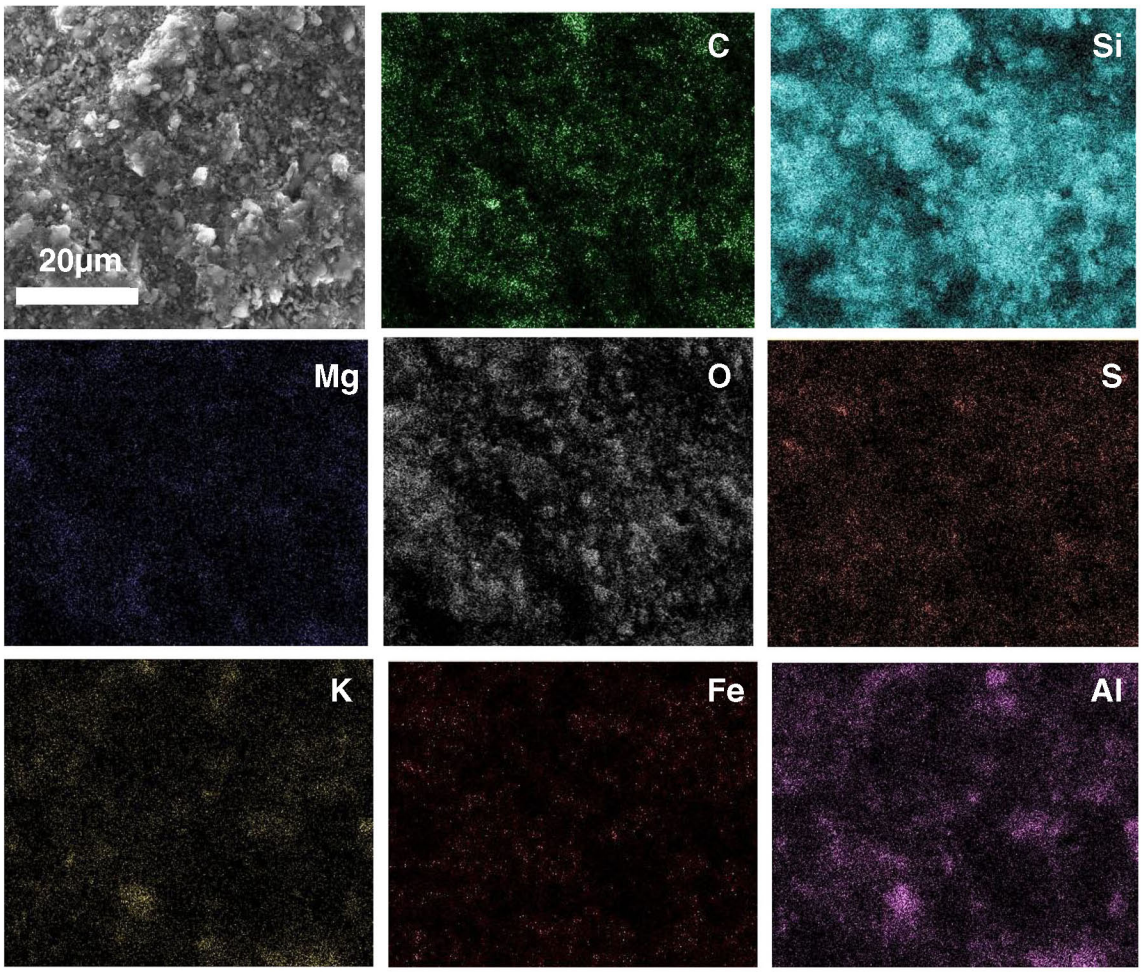

Fig. 3 SEM micrographs of shungite and maps of distribution of elements on the surface of shungite

using a Perkin-Elmer thermogravimetric analyzers (TGA) instruments, with oxygen as purge gas at a flow rate of 20 ml min^{-1}. Samples were heated from 25 to 900 °C at a rate of 10 °C min^{-1}.

Electrochemical cells were assembled with shungite and commercial carbon as working electrodes, lithium foil as counter electrode, and $LiPF_6$ 1 M in ethylene carbonate-dimethyl carbonate (EC:DMC) 1:1 *w/w* as electrolyte. All electrochemical tests were performed at room temperature. The cells were galvanostatically cycled, at 0.5 C, in the potential range 0.0 to 1.5 V and 0.0 to 2.5 V vs. Li/Li for commercial carbon and shungite electrodes, respectively, using a VMP3 multi-channel galvonostat-potentiostat-EIS (Bio-Logic).

EIS measurements were performed using a superimposed AC voltage amplitude of 5 mV in the frequency range of 0.1 to

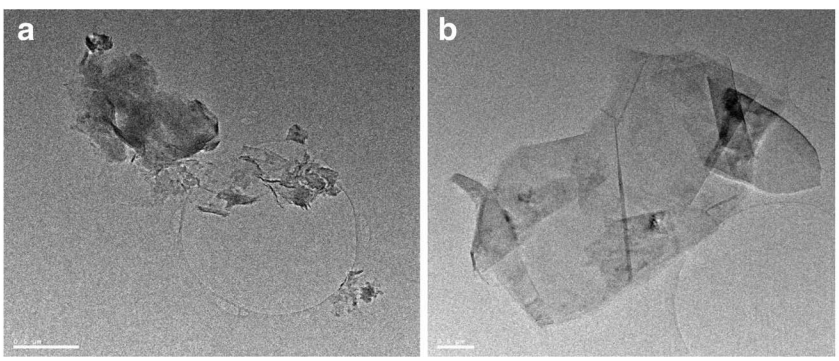

Fig. 4 Low-magnification TEM image of **a** shungite and **b** commercial carbon

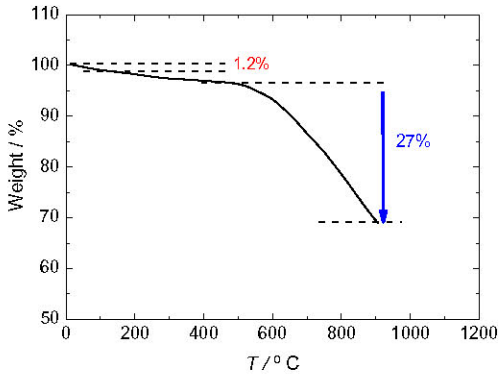

Fig. 5 Thermogravimetric plot of the shungite sample

100,000 Hz. Then, the rate capability performance of the cells was studied at different C rates (0.25, 0.5, 1, 2, 5, and 10 C) during 4 cycles.

Results and discussion

Characterization of samples

The shungite and carbon were analyzed by X-ray diffraction. The XRD pattern (Fig. 1) exhibits a crystalline structure. The wide peaks at about 26° and 54° are attributed to the carbon layer (Fig. 1a), and the peak at 27° corresponds to the SiO_2 (Fig. 1b). From the phase quantification for the shungite sample, it is possible to find a 95 % relation to SiO_2 and 5 % to carbon. These results can be explained taking into account that the amount of carbon in the shungite sample is mostly amorphous giving rise to a diffraction result with less carbon content.

Figure 2 shows SEM images (×10,000) and the corresponding EDS analysis of shungite and commercial carbon samples. Shungite samples exhibit morphology of plate shape type; however, the commercial carbon materials present a kind of thin sheet plate structures. The shungite EDS spectrum shows a composition of approximately 40 % in mass of carbon and a small concentration of some impurities, less than 1 % (Table 1).

Results of EDS elemental mapping for the shungite are shown in Fig. 3. The bright regions correspond to the presence of elements carbon (green), silicon (cyan), magnesium (blue), oxygen (white), sulfur (orange), potassium (yellow), iron (red), and aluminum (magenta), respectively. The result indicates that elements are distributed uniformly in the minerals.

The microstructure was investigated by TEM. The TEM micrographs at low magnification (Fig. 4) show, in both samples, agglomerated regions. As can be seen, the shungite samples are characterized by particles of smaller size than commercial carbon material, a fact that is in good agreement with SEM results.

The TGA curves of Fig. 5 indicate the existence of two different weight losses. The first loss, visible in the temperature range 25–130 °C (1.2 %), was associated to the evaporation of residual small molecules, such as water, alcohol, and ethanol [17]. The sample mass remained invariable until 500 °C. Above this temperature, a second degradation was detected, with a weight loss of 27 % that could be related to the carbon combustion.

Electrochemical characterization

The kinetics of lithium intercalation in any composite electrode materials can be studied using cyclic voltammograms (CV). Figure 6 shows the CV peaks corresponding to insertion and disinsertion of lithium.

Figure 7a displays the discharge capacities vs. the cycle number. In this paper, the capacity was calculated as a function of the total amount (grams) of the shungite. During the first cycle, the discharge capacities of commercial carbon and shungite samples were about 200 and 110 mA h g^{-1}, respectively. It is worth noting that these capacity values were calculated considering the worst assumption condition. Initially, the commercial carbon samples exhibited higher discharge capacity, than shungite electrodes. The discharge capacity of the commercial carbon electrodes increases with cycling and after the 4th cycle remains around a constant value of

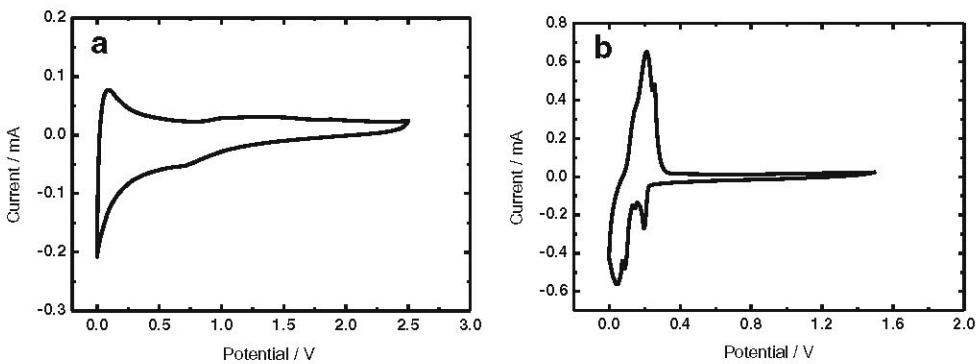

Fig. 6 Cyclic voltammograms at 0.1 mV s^{-1}, in $LiPF_6$ 1 M in EC:DMC 1:1 *w/w*: **a** shungite electrode and **b** commercial carbon electrode

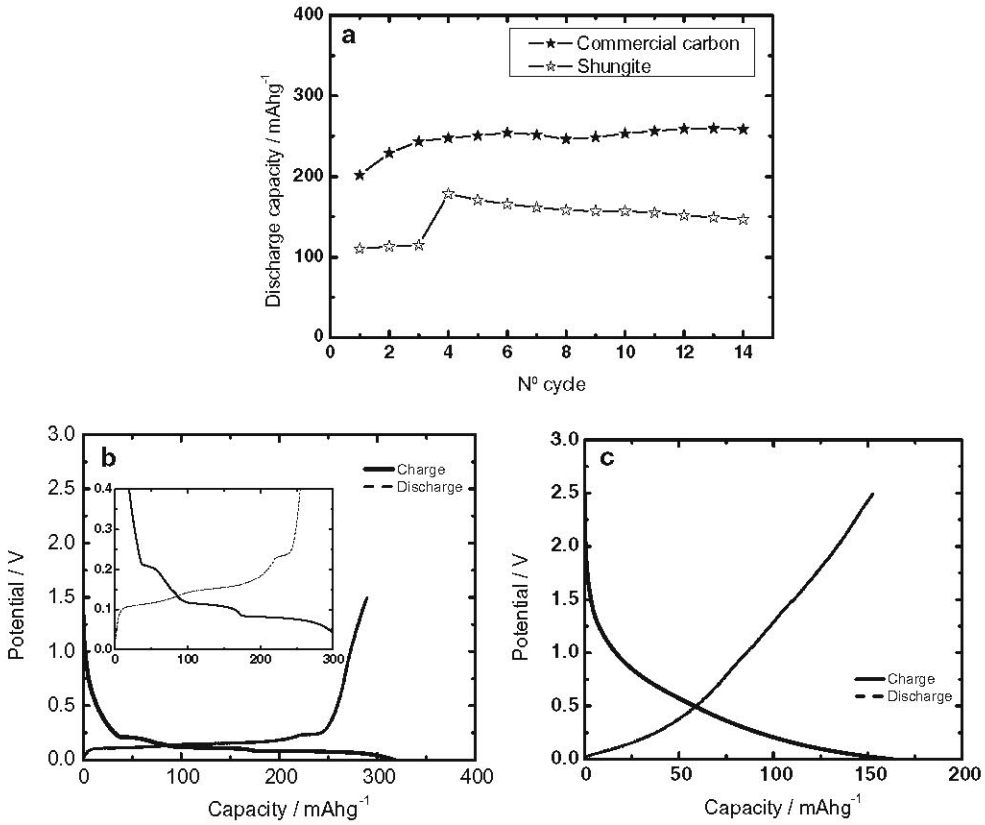

Fig. 7 **a** Discharge capacity vs. cycle number. Charge-discharge profiles of **b** commercial carbon electrode and **c** shungite electrode

250 mA h g ^{1}. After the 4th cycle, the shungite electrodes present, with increasing cycle number, a small decrease in the discharge capacity values.

The charge-discharge profiles of studied electrodes are illustrated in Fig. 7b, c. They were obtained at 0.5-C rate, at cut-off potential ranges of 2.50–0.00 V and 1.5–0.0 V, for shungite and commercial carbon, respectively. A magnification, in the 0.0–0.4-V potential range, was made to better observe the plateau. All observed plateau potentials in the charge-discharge profiles are in a good agreement with CV peaks shown in Fig. 6.

The discharge capacities, after 14th cycles, were 146 and 258 mA h g ^{1} for shungite and commercial carbon electrode, respectively. The specific discharge capacity of commercial carbon was higher than that for shungite carbon electrodes.

Figure 8 shows the plot of different discharge capacities vs. number of cycles, at different discharge rates. The shungite electrodes show a decrease of discharge capacity values, when discharge current (I) increases. However, the commercial carbon electrodes exhibited that the capacity is slightly affected by the increase in current. Consequently, taking into consideration the rate capability results, it is apparent that commercial carbon electrodes present better electrochemical performance.

Nyquist diagrams corresponding to the studied samples are presented in Fig. 9. The diagrams show, at the high-frequency region, a phase angle close to 45° that is characteristic of a porous structure. The high-frequency semicircle is due to the formation of the solid-electrolyte interphase (SEI) film. The capacitive loop, at the intermediate range of frequencies, is associated with the parallel connection of the electrical double layer (C_{dl}), the charge transfer resistance (R_t) related to the intercalation/deintercalation of lithium ions. For lower frequencies, a diffusional impedance type is shown. For both electrodes, impedance values increase with increasing state

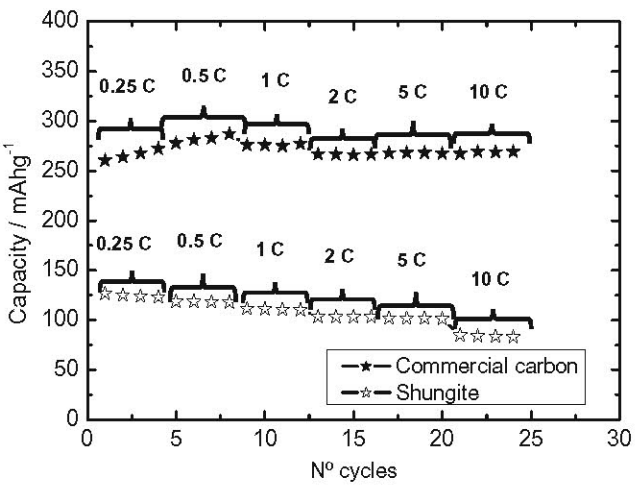

Fig. 8 Discharge capacity vs. N° cycle, at different current discharge

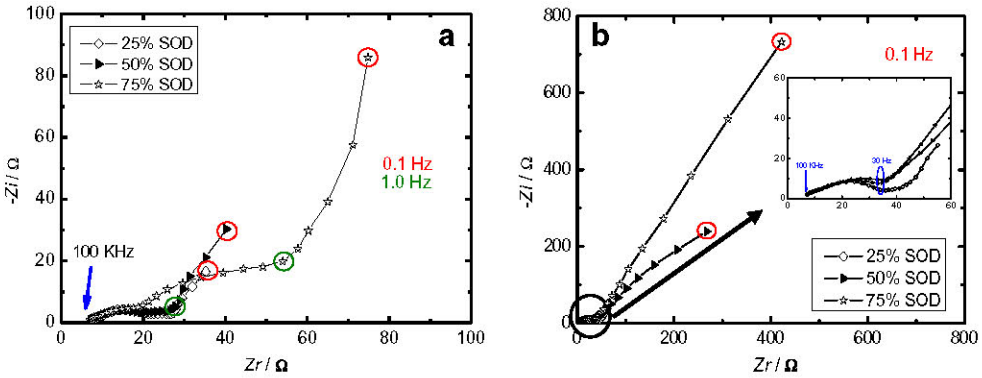

Fig. 9 Nyquist's diagrams for **a** commercial carbon electrode and **b** shungite electrode

of discharge (% SOD). The shungite electrode exhibited higher impedance values. It is apparent that resistance values for the high-frequency loop are lower for shungite samples that could be related to the presence of a SEI with poor passivating properties.

Conclusions

The carbon and shungite anodes were investigated employing electrochemical techniques, such as charge-discharge cycling, electrochemical impedance spectroscopy, cycling voltammetric, as well as physical-chemical analysis. The morphological characterization of the shungite revealed that the elements are distributed uniformly in the mineral. The electrochemical tests exhibited that the carbon electrodes show better capacity than the shungite composite electrodes, being this fact probably due to the complex composition of the mineral. Accordingly, it was observed that at 10th cycle, that the discharge capacity values were 253 and 156 mA h g ^{1} for carbon and shungite electrodes, respectively. It should be noted that if the lithiation process is considered as taking place only in a part of the shungite material, the calculated capacity values will be higher.

Acknowledgments This work was supported by the Agencia Nacional de Promoción Científica (ANPCyT), the Consejo Nacional de Investigaciones Científicas y Técnicas (CONICET), and the Universidad Nacional de La Plata. The Czech partners were supported by the Centre of Research and Utilization of Renewable Power Sources (CVVOZE) with financial assistance by the Ministry of Education program NPU 1 (N° LO1210).

References

1. Weydanz W, Wohlfahrt-Mehrens M, Huggins R (1999) A room temperature study of the binary lithium–silicon and the ternary lithium–chromium–silicon system for use in rechargeable lithium batteries. J Power Sources 81-82:237–242
2. Guo ZP, Wang JZ, Liu HK, Dou SX (2005) Study of silicon/polypyrrole composite as anode materials for Li-ion batteries. J Power Sources 146:448–451
3. Kasavajjula U, Wang C, Appleby AJ (2007) Nano-and bulk-silicon-based insertion anodes for lithium-ion secondary cells. J Power Sources 163:1003–1039
4. Wu H, Cui Y (2012) Designing nanostructured Si anodes for high energy lithium ion batteries. NanoToday 7:414–429
5. Holzapfel M, Buqa H, Hardwick LJ, Hahn M, Würsig A, Scheifele NP, Kötz R, Veit C, Petrat F-M (2006) Nano silicon for lithium-ion batteries. Electrochim Acta 52:973–978
6. Ryu JH, Kim JW, Sung Y-E, Oh SM (2004) Failure modes of silicon powder negative electrode in lithium secondary batteries. Electrochem Solid-State Lett 7:A306
7. Liu HK, Guo ZP, Wang JZ, Konstantinov K (2010) Si-based anode materials for lithium rechargeable batteries. J Mater Chem 20: 10055
8. Yoon YS, Jee SH, Lee SH, Nam SC (2011) Nano Si-coated graphite composite anode synthesized by semi-mass production ball milling for lithium secondary batteries. Surf Coat Technol 206:553–558
9. Tao H-C, Huang M, Fan L-Z, Qu X (2013) Effect of nitrogen on the electrochemical performance of core–shell structured Si/C nanocomposites as anode materials for Li-ion batteries. Electrochim Acta 89:394–399
10. Wu J, Zhu Z, Zhang H, Fu H, Li H, Wang A, Zhang H, Hu Z (2014) A novel nano-structured interpenetrating phase composite of silicon/graphite–tin for lithium-ion rechargeable batteries anode materials. J Alloys Compd 596:86–91
11. Yang J, Wang BF, Wang K, Liu Y, Xie JY, Wen ZS (2003) Si/C composites for high capacity lithium storage materials. Electrochem Solid-State Lett 6:A154
12. Zhang L, Song X, Wang F, Hu Q, Sun Z, Yang S, Wang L, Sun S (2012) The electrochemical properties of Al–Si–Ni alloys composed of nanocrystal and metallic glass for lithium-ion battery anodes. J Solid State Electrochem 16:2159–2167
13. Park J-B, Lee K-H, Jeon Y-J, Lim S-H, Lee S-M (2014) Si/C composite lithium-ion battery anodes synthesized using silicon nanoparticles from porous silicon. Electrochim Acta 133:73–81
14. Endo M, Kim C, Nishimura K, Fujino T, Miyashita K (2000) Recent development of carbon materials for Li ion batteries. Carbon 38:183–197
15. Maroni F, Raccichini R, Birrozzi A, Carbonari G, Tossici R, Croce F, Marassi R (2014) Graphene/silicon nanocomposite anode with enhanced electrochemical stability for lithium-ion battery applications. J Power Sources 269:873–882
16. Yeh T-S, Wu Y-S, Lee Y-H (2011) Graphitization of unburned carbon from oil-fired fly ash applied for anode materials of high power lithium ion batteries. Mater Chem Phys 130:309–315
17. Jianguo L, Gaoping G, Chuanwei Y (2006) Enhancement of the erosion–corrosion resistance of Dacromet with hybrid SiO2 sol–gel. Surf Coat Technol 200:4967–4975